

Nonlinear inverse solution by the look-up table method for Risley-prism-based scanner

ANHU LI^{*}, WANSONG SUN, XINJIAN GAO

School of Mechanical Engineering, Tongji University,
4800 Caoan Road, Shanghai, 201804, China

^{*}Corresponding author: lah@tongji.edu.cn

A pair of rotation Risley prisms can perform superior optical pointing and tracking functions with large visual field and high accuracy. Crucial to the function implementation are the nonlinear inverse solutions to the double-prism orientation angles for tracking a given target trajectory. In the paper, a novel look-up table method is proposed to solve this problem. Because there are two groups of solutions to the rotation angles achieved from an arbitrary target point, a “jump” phenomenon occurs and generates the discontinuous curves of multi-group rotation angle solutions. According to the mapping relation between the coordinate values of the target point and the corresponding rotation angles of two prisms, we can establish the continuous solution curves by adding constraints and employing an optimization algorithm. Experimental results validate the obtained inverse solutions applicable to scan a trajectory close to the given one within an error threshold. The proposed look-up table method can provide foundation for the continuous control of the Risley-prism-based scanner in its inverse applications.

Keywords: Risley prism, look-up table method, inverse solution, scanner.

1. Introduction

A pair of rotation Risley prisms, which can perform superior optical pointing and tracking functions, appears to be the most promising solution in the fields of free-space laser communications [1], laser radar [2], optical switches [3], laser scanning and other optical engineering [4–7]. In general, there are two basic problems encountered in the application of double-prism systems, namely the forward solution and the inverse one [8, 9]. The forward solution answers how to solve the deviation direction of the laser beam emerging from the system according to the given orientations of two prisms. And the inverse one establishes a solution to the rotation angles of two prisms under the conditions of the given emergent beam deviation angles. Previous researches [10–14] have established approximate solutions to the forward and inverse problems. However, without considering the prism thickness and the spacing distance between two prisms,

the previous approaches are more valuable for the far-field applications rather than the near-field cases due to the scanning errors of the trajectory.

In 2011, YAJUN LI [10] took a two-step method to solve the rotation angles of double prisms according to a known emergent beam vector. But without considering the prism thickness and spacing parameter between two prisms, the available scan region solved by the two-step method is smaller than the actual scan region [10, 12, 13]. Moreover, with this approximate solution it is difficult to meet the performance requirements in high-accuracy scanning and tracking cases. In 2015, we proposed an inverse solution with iterative refinement by a forward solution to solve the inverse problem for a given target point [15], but the available scan region for the iterative method is also smaller than the actual scan region because it is an improved algorithm based on the two-step method. Therefore, there is one or another limit in the existing methods. On the other hand, for a given target point, there are correspondingly two groups of rotation angle solutions, so how to select the appropriate rotation angle solution to keep the rotation angle solutions continuous and eliminate the “jump” phenomenon for a continuous target trajectory is an important issue.

In this paper, based on our previous researches [13–15], a novel look-up table method is proposed to obtain the inverse solutions of the rotation double-prism system for a given target point, which can further establish a mapping relation from an arbitrary given target trajectory to the rotation angle curves of two prisms in the whole actual scan region. The approximate rotation angle solutions can be solved through searching a look-up table for the point nearest to the target point by the proposed approach. And an optimization is performed to avoid the “jump” phenomenon between two groups of solutions. Therefore, the continuous control of rotation angles can be carried out for the inverse tracking and scanning applications. The paper is arranged as follows: first the coordinate expressions of the refractive beam through each surface of two prisms are established, then the main process of the look-up table method is investigated and the factors affecting the look-up table implementation are discussed; and finally, a feasible optimization method as well as the experimental validation are performed.

2. Beam scanning principle of rotation double prisms

The schematic diagram of two identical rotating prisms is described in Fig. 1a. The laser beam propagates through prism Π_1 and prism Π_2 in sequence, and finally projects onto the optical receiving screen. The rotation speeds of prism Π_1 and prism Π_2 are set to ω_1 and ω_2 , respectively. With different rotation speed ratios of two prisms ω_2/ω_1 , various scanning patterns of the refractive beam can be formed on the screen [8].

For far-field applications, the impact of the system parameters on a scanning trajectory can be ignored, so the beam is considered to exit from the central point on the emergent surface of prism Π_2 . Then an approximate scanning trajectory is obtained. However, in fact, the emergent beam will deviate from this central point. For near-field applications, the system parameters will greatly influence the accuracy of the

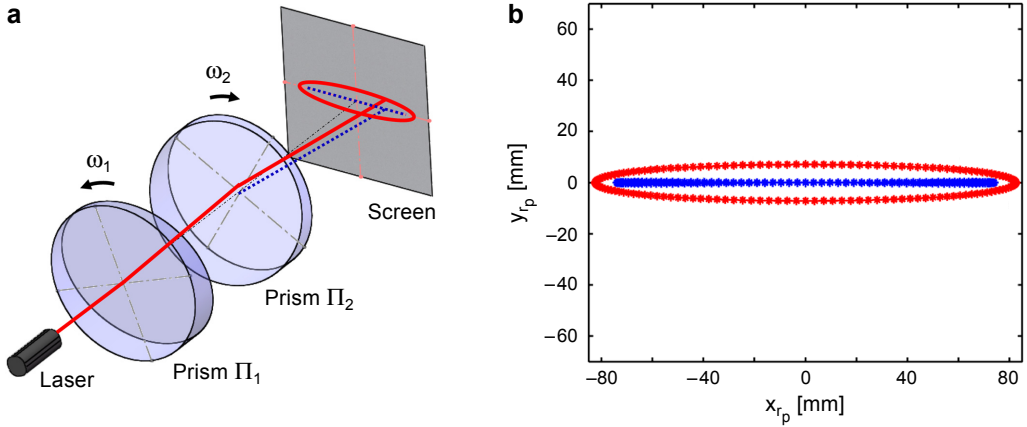


Fig. 1. Schematic diagram of rotation Risley-prism-based scanning system. Optical scanning principle of rotation double prisms (a), and the scanning patterns on receiving screen when $\omega_2 = -\omega_1$ (b).

approximate scanning trajectory, and the deviation distance on the emergent surface of prism Π_2 cannot be neglected. Then an exact scanning trajectory is achieved. For example, when two prisms rotate with the same speed but in the opposite direction, namely $\omega_2 = -\omega_1$, a near straight line and an ellipse can be regarded as the approximate and the exact trajectory, respectively, as the dashed line and the continuous line shown in Fig. 1a. In Figure 1b, the scanning trajectories in Fig. 1a are further illustrated on a coordinate paper.

As shown in Fig. 2, the propagation process of a refractive beam through the rotation double-prism system is schematically described. The thickness of the prisms at the central position is set to d , the rotation angles of prism Π_1 and prism Π_2 are θ_{r_1} and θ_{r_2} , respectively, the wedge angles of two prisms are both set to α , and the refractive indexes of two prisms are n . The distance between the surface 11 of prism Π_1 and the surface 22 of prism Π_2 is D_1 , and the distance between the surface 22 and the receiving screen is set to D_2 . According to the vector refraction theorem [16, 17], the equation

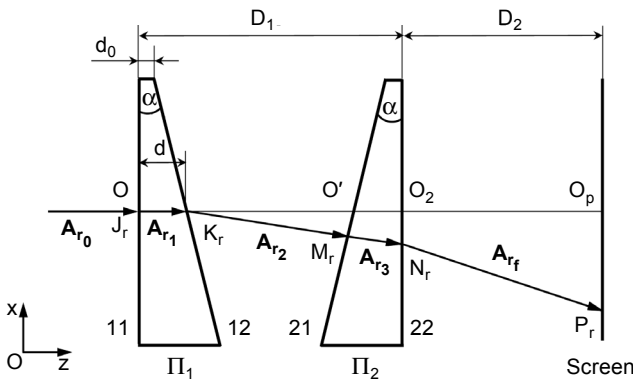


Fig. 2. Schematic description of refractive beam through a pair of rotation Risley prisms.

expressions of the surface 11, 12, 21, 22 and the receiving screen can be respectively written as:

$$z = 0 \quad (1a)$$

$$\cos(\theta_{r_1})\sin(\alpha)x + \sin(\theta_{r_1})\sin(\alpha)y + \cos(\alpha)(z - d) = 0 \quad (1b)$$

$$-\cos(\theta_{r_2})\sin(\alpha)x - \sin(\theta_{r_2})\sin(\alpha)y + \cos(\alpha)[z - (D_1 - d)] = 0 \quad (1c)$$

$$z = D_1 \quad (1d)$$

$$z = D_1 + D_2 \quad (1e)$$

and the normal vectors of the surface 11, 12, 21 and 22, denoted by \mathbf{N}_{11} , \mathbf{N}_{12} , \mathbf{N}_{21} and \mathbf{N}_{22} , are sequentially expressed as

$$\mathbf{N}_{11} = (0, 0, 1)^T \quad (2a)$$

$$\mathbf{N}_{12} = (\cos(\theta_{r_1})\sin(\alpha), \sin(\theta_{r_1})\sin(\alpha), \cos(\alpha))^T \quad (2b)$$

$$\mathbf{N}_{21} = (-\cos(\theta_{r_2})\sin(\alpha), -\sin(\theta_{r_2})\sin(\alpha), \cos(\alpha))^T \quad (2c)$$

$$\mathbf{N}_{22} = (0, 0, 1)^T \quad (2d)$$

Based on the above derivation, the interaction points of the beam through the double-prism system can be calculated. Given the incident beam vector of prism II_1 is $\mathbf{A}_{r_0} = (x_{r_0}, y_{r_0}, z_{r_0})$, the refractive beam vectors after the surface 11, 12, 21 and 22 are $\mathbf{A}_{r_1} = (x_{r_1}, y_{r_1}, z_{r_1})$, $\mathbf{A}_{r_2} = (x_{r_2}, y_{r_2}, z_{r_2})$, $\mathbf{A}_{r_3} = (x_{r_3}, y_{r_3}, z_{r_3})$ and $\mathbf{A}_{r_f} = (x_{r_f}, y_{r_f}, z_{r_f})$, respectively. So according to the intersection point $\mathbf{J}_r(x_{r_j}, y_{r_j}, z_{r_j})$ of the incident beam on the surface 11, the coordinate values of each intersection point $\mathbf{K}_r(x_{r_k}, y_{r_k}, z_{r_k})$, $\mathbf{M}_r(x_{r_m}, y_{r_m}, z_{r_m})$, $\mathbf{N}_r(x_{r_n}, y_{r_n}, z_{r_n})$ and $\mathbf{P}_r(x_{r_p}, y_{r_p}, z_{r_p})$ of the refractive beam on the surface 12, 21, 22 and the screen can be respectively expressed as follows:

$$\begin{pmatrix} x_{r_k} \\ y_{r_k} \\ z_{r_k} \end{pmatrix} = t_{c_1} \begin{pmatrix} x_{r_1} \\ y_{r_1} \\ z_{r_1} \end{pmatrix} + \begin{pmatrix} x_{r_j} \\ y_{r_j} \\ z_{r_j} \end{pmatrix} \quad (3)$$

$$\begin{pmatrix} x_{r_m} \\ y_{r_m} \\ z_{r_m} \end{pmatrix} = t_{c_2} \begin{pmatrix} x_{r_2} \\ y_{r_2} \\ z_{r_2} \end{pmatrix} + \begin{pmatrix} x_{r_k} \\ y_{r_k} \\ z_{r_k} \end{pmatrix} \quad (4)$$

$$\begin{pmatrix} x_{r_n} \\ y_{r_n} \\ z_{r_n} \end{pmatrix} = t_{c_3} \begin{pmatrix} x_{r_3} \\ y_{r_3} \\ z_{r_3} \end{pmatrix} + \begin{pmatrix} x_{r_m} \\ y_{r_m} \\ z_{r_m} \end{pmatrix} \tag{5}$$

$$\begin{pmatrix} x_{r_p} \\ y_{r_p} \\ z_{r_p} \end{pmatrix} = t_{c_4} \begin{pmatrix} x_{r_f} \\ y_{r_f} \\ z_{r_f} \end{pmatrix} + \begin{pmatrix} x_{r_n} \\ y_{r_n} \\ z_{r_n} \end{pmatrix} \tag{6}$$

where

$$t_{c_1} = \frac{-\cos(\theta_{r_1})\sin(\alpha)x_{r_j} - \sin(\theta_{r_1})\sin(\alpha)y_{r_j} - \cos(\alpha)(z_{r_j} - d)}{\cos(\theta_{r_1})\sin(\alpha)x_{r_1} + \sin(\theta_{r_1})\sin(\alpha)y_{r_1} + \cos(\alpha)z_{r_1}} \tag{7a}$$

$$t_{c_2} = \frac{\cos(\theta_{r_2})\sin(\alpha)x_{r_k} + \sin(\theta_{r_2})\sin(\alpha)y_{r_k} - \cos(\alpha)[z_k - (D_1 - d)]}{-\cos(\theta_{r_2})\sin(\alpha)x_{r_2} - \sin(\theta_{r_2})\sin(\alpha)y_{r_2} + \cos(\alpha)z_{r_2}} \tag{7b}$$

$$t_{c_3} = \frac{D_1 - z_{r_m}}{z_{r_3}} \tag{7c}$$

$$t_{c_4} = \frac{D_1 + D_2 - z_{r_n}}{z_{r_f}} = \frac{D_2}{z_{r_f}} \tag{7d}$$

3. Look-up table method for the inverse solution

3.1. Process of the look-up table method

Solving the inverse problem with a look-up table method is to establish the mapping relation from the coordinates of a scanning point to the corresponding rotation angles of two prisms. The process of the look-up table method can be summarized as follows.

Establish a table. According to the analysis results in Section 2, the coordinate values of the intersection point P_r are determined by the rotation angles θ_{r_1} and θ_{r_2} , the wedge angle α , the refractive index n , the central thickness d , and the distance D_1 and D_2 . Therefore, for different applications of a double-prism system, a series of reasonable structure parameters should be determined firstly, as well as the rotation range from 0 to 360°. According to the requirement of scanning accuracy, the rotation step angle θ_{tre} of two prisms can be calculated, so the rotation angles of two prisms can be divided into $360^\circ/\theta_{tre}$. Based on the formulas (3) to (6), the coordinate values $(x_{r_p}, y_{r_p}, z_{r_p})$ of the beam scanning point on the screen can be obtained relative to the

corresponding group data $(\theta_{r_1}, \theta_{r_2})$ with a resolution θ_{tre} . Then a database that consists of $(\theta_{r_1}, \theta_{r_2})$ and $(x_{r_p}, y_{r_p}, z_{r_p})$ can be established for a specified rotation double-prism system. Theoretically, as the step angle θ_{tre} decreases, the size of the look-up table will be enlarged while the solution accuracy can be well improved.

Look up the table. For a given target trajectory $y = f(x)$, the coordinate values $(X_{r_p}, Y_{r_p}, Z_{r_p})$ of P_r on the trajectory curve can be calculated according to a specified sampling frequency (where $Z_{r_p} = D_1 + D_2$). The points nearest to the target points within the established database can be sought according to the requirements of a minimal target position error

$$\min(\Delta) = \min\left(\sqrt{(X_{r_p} - x_{r_p})^2 + (Y_{r_p} - y_{r_p})^2 + (Z_{r_p} - z_{r_p})^2}\right) \quad (8)$$

and then the computer can automatically seek the corresponding rotation angles $(\theta_{r_1}, \theta_{r_2})$ with respect to $(x_{r_p}, y_{r_p}, z_{r_p})$ in the database, which can be used as the approximate inverse solutions to the rotation double prisms to meet the scanning and tracking requirements.

Data processing. Because the rotation angles $(\theta_{r_1}, \theta_{r_2})$ obtained from the look-up table are serial discrete values, a continuous rotation angle curve is finally drawn by function interpolation.

3.2. Inverse solution examples for a double-prism system by the look-up table method

As shown in Fig. 2, the prism parameters and structural parameters are set as follows: the wedge angles α are 10° , the refractive indexes n are 1.517, the clear apertures D_p are 80 mm, the thicknesses d_0 of the thinnest end are 5 mm, the distance D_1 is 100 mm, the distance D_2 is 400 mm, and the rotation angle ranges of two prisms are 0 to 360° . The rotation step angles of two prisms are set to 0.1° , so the rotation angles can be divided into 3600 groups within the whole rotation angle range. The coordinate value Z is a constant, namely $Z_{r_p} = D_1 + D_2 = 500$ mm. By the meshgrid function in Matlab program, the matrix of angle group combination with the size of 3600×3600 can be obtained, and the corresponding coordinate values (x_{r_p}, y_{r_p}) calculated by the formula (6) can be written into the database. So a look-up table is produced with the data size $3600 \times 3600 \times 2 = 2.592 \times 10^7$.

Taking a target trajectory of cardioid

$$\begin{cases} x = 20 \left[2 \sin(\theta) - \sin(2\theta) \right] \\ y = 20 \left[2 \cos(\theta) - \cos(2\theta) \right] \end{cases}, \quad 0 \leq \theta \leq 2\pi \quad (9)$$

as an example, the scanning period time is set to 10 seconds with a uniform scanning speed, and the sampling point number is 64 over the whole tracking process. Obvious-

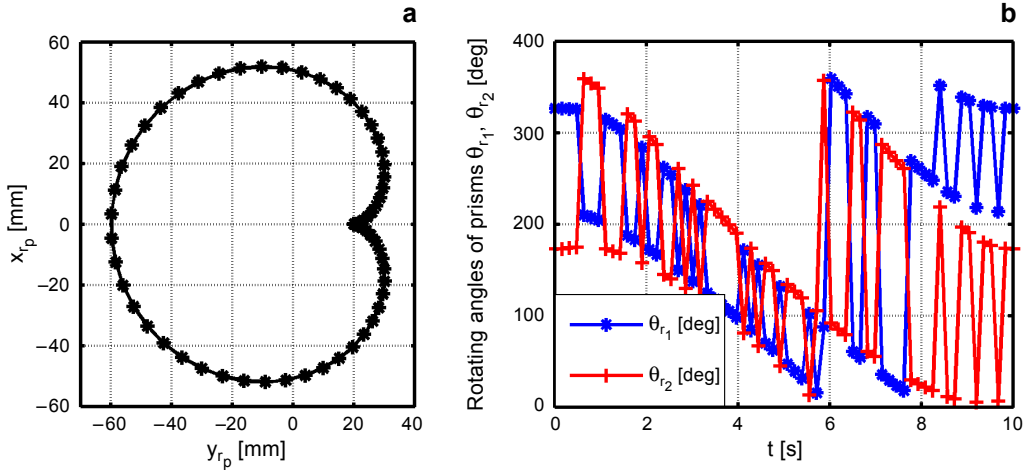


Fig. 3. An application example: cardioid target trajectory (a), and rotation angle curves of double prisms with time change (b).

ly, in practical applications, the more sampling points we select, the higher scanning accuracy we can achieve. First, the coordinate values (X_{r_p}, Y_{r_p}) of each sampling point on the target trajectory can be calculated. Then through calculating the minimal error $\min(\Delta)$ (see Eq. (8)) between the points in the database and the desired sampling point, the row number N and column number M corresponding to the value (x_{r_p}, y_{r_p}) in database are obtained and returned. Therefore the corresponding $\theta_{r_1} = \theta_{\text{tre}}(N - 1)$ and $\theta_{r_2} = \theta_{\text{tre}}(M - 1)$ are found, and a series of discrete values of rotation angles can be input into the matrix $(\theta_{r_1}, \theta_{r_2})$, which are the approximate solutions to rotation angles for the corresponding sampling points. Finally, the discrete points in the matrix $(\theta_{r_1}, \theta_{r_2})$ are fitted through a segmental lower-order interpolation, and the approximate rotation angle curves of rotation double prisms come into being.

By the look-up table method, 64 sampling points in Fig. 3a are selected, and rotation angles of two prisms corresponding to each sampling point can be searched. Substitute the rotation angles into the formulas (3) to (6) to solve the actual beam scanning points on the screen, and the positions of these scanning points can be compared with those of the desired sampling points on the origin function curve. As a result, the distance error Δ range from 0.002346 to 0.040524 mm.

4. Optimization of the look-up table method

4.1. Discussion on the “jump” phenomenon

As shown in Fig. 3b, a discontinuity problem of the rotation angle curves occurs, that is, the corresponding rotation angles change greatly between two adjacent sampling points, which is called the “jump” phenomenon. Consequently, the response time will be too long to synchronously track the target even if it moves slightly. The reason for

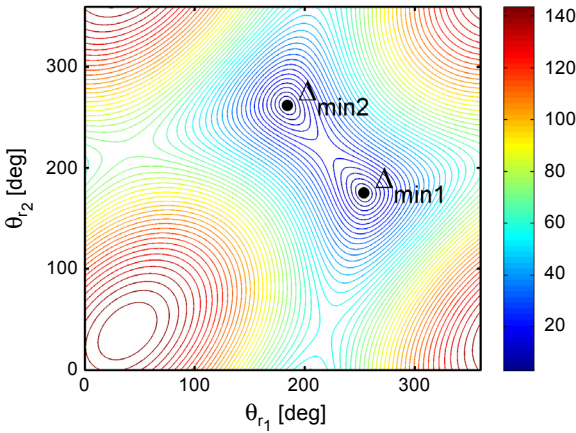


Fig. 4. Contour map of the errors Δ.

this phenomenon is that the inverse solution of the rotation double-prism system is not unique. For a given target point, at least two groups of rotation angles can be sought to meet the value of minimum Δ requirement in theory.

For instance, in order to track the target point (50 mm, 40 mm) by the look-up table method with a step angle 0.5°, the errors $\Delta = [(X_{rp} - x_{rp})^2 + (Y_{rp} - y_{rp})^2]^{1/2}$ between all the points in the database and the desired target points are calculated firstly, and then the contour map of the errors Δ is shown in Fig. 4. Evidently, there are two minimum Δ of the errors, which illustrates that two groups of rotation angles can be found for the same target point in theory. As a result, the “jump” phenomenon of the rotation angle curves occurs.

4.1.1. Impact of the rotation step angle

As shown in Table 1, using different rotation step angles to establish look-up tables, the rotation angles (θ_{r1}, θ_{r2}) at the extreme point and the database size both change. When the step angle 1° or 0.1° is used, the value of minimum Δ is 0.1736 or 0.0283 mm located at the extreme point 2, while the value of minimum Δ is 0.0927 mm located at the extreme point 1 if the step angle becomes 0.5°. Thus, different step angles will affect the value of minimum Δ, as well as its position at the extreme point 1 or extreme point 2, which also further influence the selection process for different rotation angles (θ_{r1}, θ_{r2}).

T a b l e 1. Value of minimum Δ for the target point (50 mm, 40 mm).

Step angle	Database size	(θ _{r1} , θ _{r2}) at extreme point 1	Δ at extreme point 1	(θ _{r1} , θ _{r2}) at extreme point 2	Δ at extreme point 2
1.0°	360×360	(254°, 175°)	0.3948 mm	(184°, 262°)	0.1736 mm
0.5°	720×720	(253.5°, 175.5°)	0.0927 mm	(184°, 262°)	0.1736 mm
0.1°	3600×3600	(253.5°, 175.4°)	0.0345 mm	(183.8°, 262°)	0.0283 mm

4.1.2. Impacts of the target point movement

When the target point moves slightly from the origin position, the “jump” phenomenon also occurs. Taking the target point (50 mm, 41 mm) as an example, the distance error Δ can be calculated as shown in Table 2. Comparing Table 2 with Table 1, the target point is only shifted by 1 mm along the Y direction. If the step angle is set to 0.5° , the value of minimum Δ for the target point (50 mm, 40 mm) appears at the position of the extreme point 1, where $(\theta_{r_1}, \theta_{r_2}) = (253.5^\circ, 175.5^\circ)$, while the value of minimum Δ for the target point (50 mm, 41 mm) appears at the location of the extreme point 2. In other words, for even a small target position shift, two prism rotation angles still jump drastically due to the existence of two values of minimum Δ . Similarly, if the step angle is set to 0.1° , the “jump” phenomenon will also occur, which is not conducive to tracking a moving target in real time.

Table 2. Value of minimum Δ for the target point (50 mm, 41 mm).

Step angle	Database size	$(\theta_{r_1}, \theta_{r_2})$ at extreme point 1	Δ at extreme point 1	$(\theta_{r_1}, \theta_{r_2})$ at extreme point 2	Δ at extreme point 2
1.0°	360×360	$(254^\circ, 177^\circ)$	0.3304 mm	$(185^\circ, 262^\circ)$	0.1035 mm
0.5°	720×720	$(253.5^\circ, 177^\circ)$	0.1210 mm	$(185^\circ, 262^\circ)$	0.1035 mm
0.1°	3600×3600	$(253.6^\circ, 176.9^\circ)$	0.0331 mm	$(185.1^\circ, 261.8^\circ)$	0.0343 mm

As a result, with the target point movement and the different step angle selection, different rotation angle combinations will be calculated according to the minimum position distance error $\min(\Delta)$ (see Eq. (8)), which will cause the rotation angle “jump”. In order to ensure the continuity of the rotation angle curves of two prisms, a continuity combination for rotation angle values will be a reasonable choice to avoid the “jump” phenomenon.

4.2. Optimization of the look-up table method

For each target point, the rotation angle combinations corresponding to two values of minimum Δ can be solved by the look-up table method. Taking the previous rotation angle values for the previous target point as the reference to the current one, the current rotation angle values can be chosen as the optimal solution according to the principle of the minimum difference value between the previous rotation angle values and current ones. In Figures 5 and 6, the optimized results of rotation angles are obtained by the above method.

As shown in Figs. 5 and 6, the sampling point number is set to 64, and the range of position distance error is from 0.002346 to 0.0468504 mm and from 0.003096 to 0.043508 mm, respectively. Compared with the results shown in Fig. 3, the distance error Δ between the desired target point and the actual scanning one increases slightly,

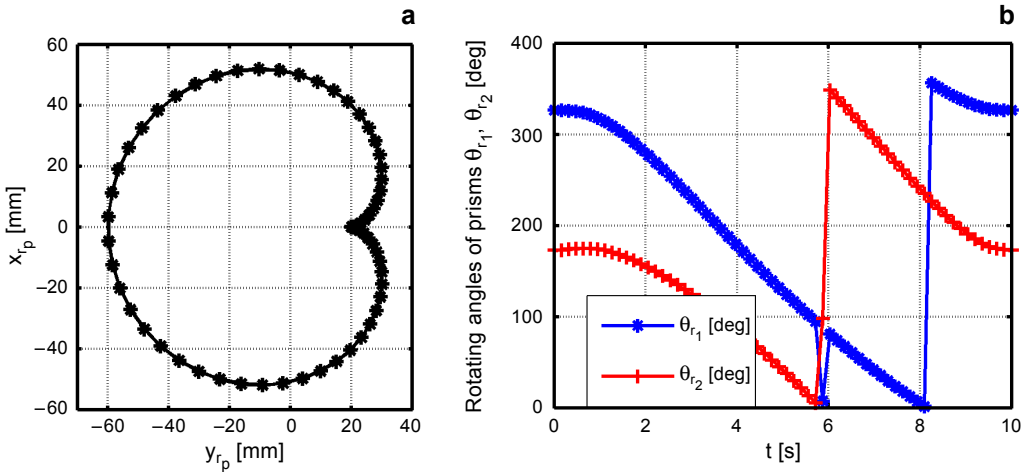


Fig. 5. Target trajectory and the corresponding rotation angle curves. The target trajectory (a cardioid) (a), and the rotation angle curves of rotation double prisms (b).

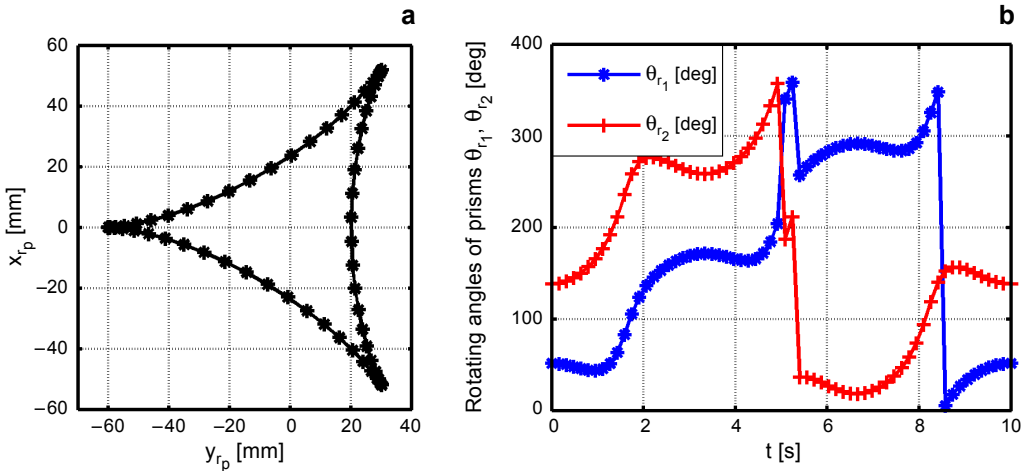


Fig. 6. Target trajectory and the corresponding rotation angle curve. The target trajectory (a deltoid) (a), and the rotation angle curves of rotation double prisms (b).

but the continuity of the rotation angles is better improved than before. However, because the rotation angles of two prisms are within 0 to 360° , when the rotation angle is close to 0 or 360° , a “jump” phenomenon still occurs. Hence, to consider the circulation problem, the following algorithm is added into the look-up table program:

- if $\theta_{r_1}(i) - \theta_{r_1}(i-1) > 180^\circ$, $\theta_{r_1}(i) = \theta_{r_1}(i) - 360^\circ$;
- if $\theta_{r_1}(i) - \theta_{r_1}(i-1) < -180^\circ$, $\theta_{r_1}(i) = \theta_{r_1}(i) + 360^\circ$.

By the above constraints together with a restriction of minimum values $\min(|\theta_{r_1}(i) - \theta_{r_1}(i-1)| + |\theta_{r_2}(i) - \theta_{r_2}(i-1)|)$, the “jump” problem during the 360° angle

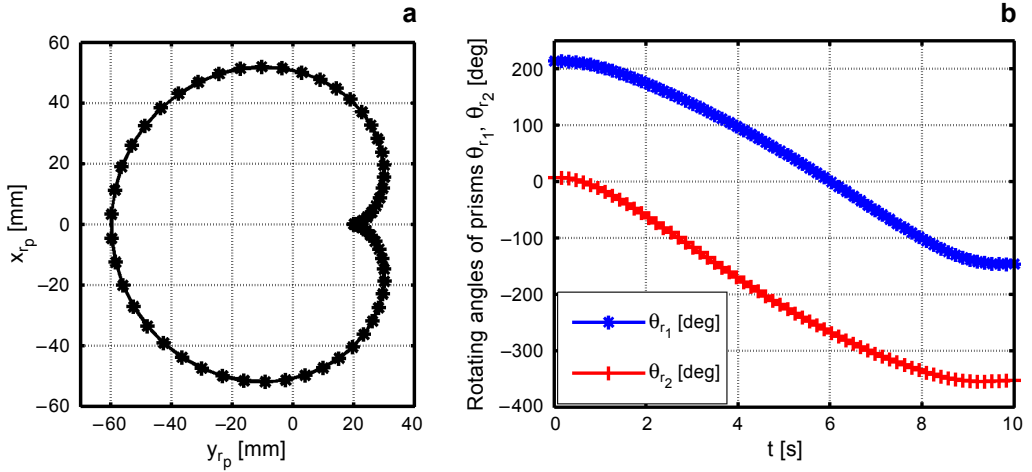


Fig. 7. Target trajectory and the corresponding rotation angle curve. The target trajectory (a cardioid) (a), and the rotation angle curves of rotation double prisms (b).

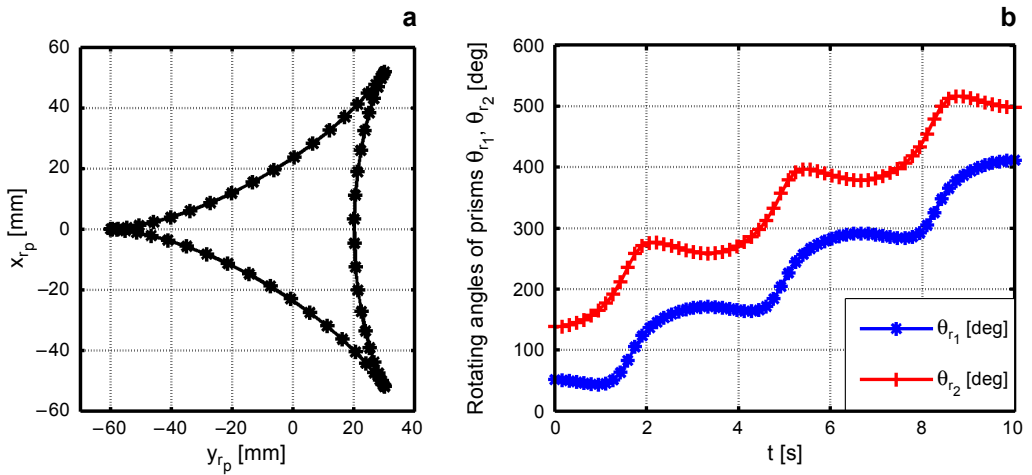


Fig. 8. Target trajectory and the corresponding rotation angle curve. The target trajectory (a deltoid) (a), and the rotation angle curves of rotation double prisms (b).

cycle can be thoroughly solved, and two continuous rotation angle curves are then established. The optimized results are described in Figs. 7 and 8.

As illustrated in Figs. 7 and 8, the sampling point numbers both are set to 64, and the range of the distance error Δ is from 0.003633 to 0.043397 mm and from 0.003098 to 0.043508 mm, respectively. Compared with Fig. 3, the optimized look-up table method causes a certain increment of the target distance error Δ , but it will improve the continuity between the adjacent rotation angles, as well as the controllability of the double-prism rotation motion.

5. Experiment

A Risley prism scanner is assembled and an experimental setup shown as Fig. 9 is developed to validate the look-up table method. The parameters of the Risley prisms are as follows: the wedge angles $\alpha = 10^\circ$, the refractive indexes $n = 1.517$, the clear apertures $D_p = 80$ mm, the thicknesses of the thinnest end $d_0 = 5$ mm, the distance between two prisms $D_1 = 100$ mm, and the distance between the surface 22 of prism I_2 and the receiving screen $D_2 = 400$ mm. The laser source with 650 nm wavelength and greater than 2.5 mW power is adjusted to be coincidence with the optical axis. The laser beam

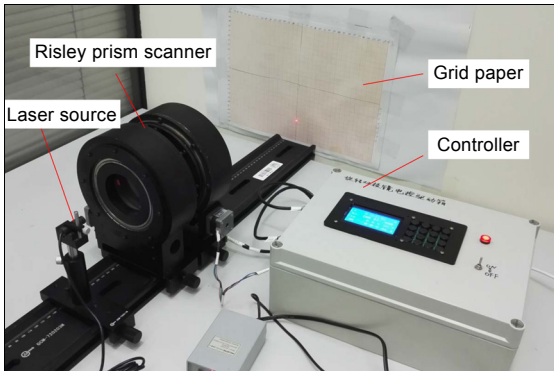


Fig. 9. Experimental setup, including Risley prism scanner, coordinate paper, controller and laser source.

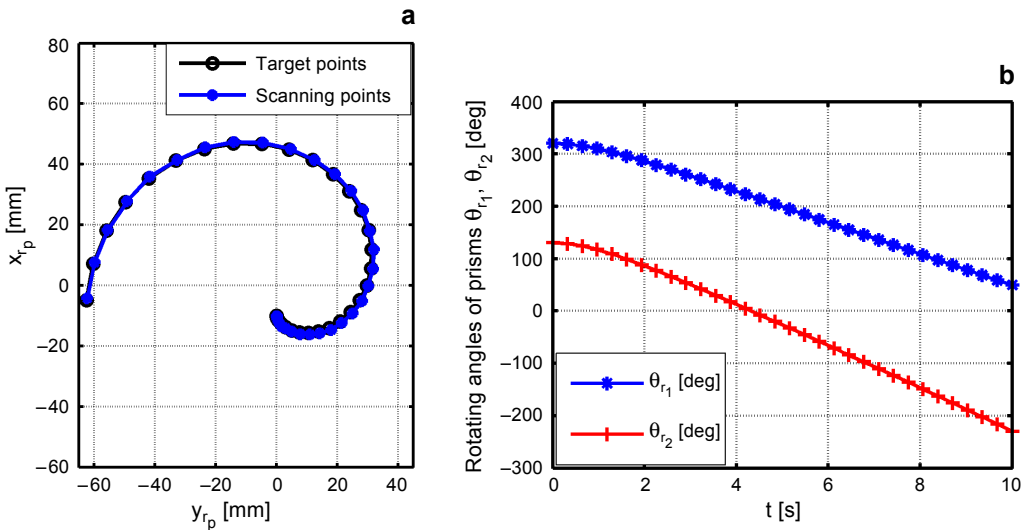


Fig. 10. Experimental results by look-up table method: target points and scanning points (a), and the rotation angle curves of double prisms corresponding to the sampling points (b).

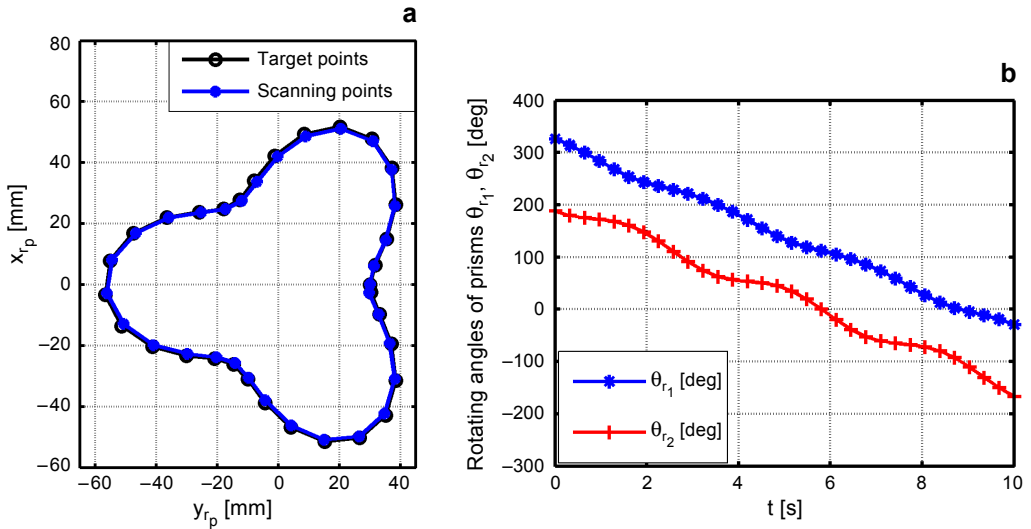


Fig. 11. Experimental results by look-up table method: target points and scanning points (a), and the rotation angle curves of double prisms corresponding to the sampling points (b).

is deflected by two prisms and hits a white coordinate paper with two dimension grids. Then the scanning point on the coordinate paper can be measured.

Two cases are investigated to validate the look-up table method. First, as shown in Fig. 10a, given an involute as the target trajectory, 32 sampling points are selected on the involute. Using the look-up table method, the corresponding rotation angles of two prisms to each sampling point are searched from the look-up table, as shown in Fig. 10b. In the experiment, two prisms are controlled to the preset rotation angles according to the rotation angle curves. The spot positions of the deflected laser beam on the coordinate paper are measured. Consequently, the actual scanning points are obtained as shown in Fig. 10a. Similarly, for the target trajectory in Fig. 11a, the corresponding rotation angles to 32 sampling points can be solved according the look-up table method, as viewed in Fig. 11b. With the rotation of two prisms, the scanning points on the coordinate paper can also be obtained, as shown in Fig. 11a. Comparing the actual scanning points with the desired target points in Figs. 10a and 11a, two actual scanning curves basically overlap the corresponding target trajectories, which strongly validates the look-up table method.

6. Conclusions

A pair of rotation Risley prisms can produce a variety of beam trajectory patterns with different rotation speed combinations [18]. The effective control for rotation angles is a key factor that determines its application effects [11, 19]. For example, according to a given target trajectory, if the rotation angles of double prisms can be reversely solved

in time, the double prisms can be used into the passive tracking fields with high accuracy [8, 9]. In the paper, a look-up table method is proposed for the inverse solution of rotation double prisms under the condition of an arbitrary given target trajectory, and the key factors that lead to the inverse solution “jump” are discussed in detail. By adding specific constraints and using an optimization algorithm, the continuous curves of rotation angle solutions are obtained, which can effectively overcome the target loss due to the “jump” of rotation angle solutions. Furthermore, the experiment results validate the availability of the solution approach. The proposed look-up table method for the inverse solution can provide an available control avenue for rotation double prisms used in the laser passive tracking and scanning fields.

Acknowledgements – This work is supported by the National Natural Science Foundation of China (NSFC) (No. 51375347).

References

- [1] LIREN LIU, LIJUAN WANG, JIANFENG SUN, YU ZHOU, XIANGHONG ZHONG, ZHU LUAN, DE'AN LIU, AIMING YAN, NAN XU, *An integrated test-bed for PAT testing and verification of inter-satellite lasercom terminals*, Proceedings of SPIE **6709**, 2007, article 670904.
- [2] LIREN LIU, *Coherent and incoherent synthetic-aperture imaging ladars and laboratory-space experimental demonstrations*, Applied Optics **52**(4), 2013, pp. 579–599.
- [3] MARSHALL G.F., *Handbook of Optical and Laser Scanning*, Dekker, 2004.
- [4] CHENG Z., KRAUSZ F., SPIELMANN CH., *Compression of 2 mJ kilohertz laser pulses to 17.5 fs by pairing double-prism compressor: analysis and performance*, Optics Communications **201**(1–3), 2002, pp. 145–155.
- [5] DUMA V.-F., ROLLAND J.P., PODOLEANU A.G., *Perspectives of optical scanning in OCT*, Proceedings of SPIE **7556**, 2010, article 75560B.
- [6] WARGER II W.C., DiMARZIO C.A., *Dual-wedge scanning confocal reflectance microscope*, Optics Letters **32**(15), 2007, pp. 2140–2142.
- [7] GARCIA-TORALES G., STROJNIK M., PAEZ G., *Risley prisms to control wave-front tilt and displacement in a vectorial shearing interferometer*, Applied Optics **41**(7), 2002, pp. 1380–1384.
- [8] SCHITEA A., TUEF M., DUMA V.-F., VLAICU A.M., *Modeling of Risley prisms devices for exact scan patterns*, Proceedings of SPIE **8789**, 2013, article 878912.
- [9] ANHU LI, YE DING, YONGMING BIAN, LIREN LIU, *Inverse solutions for tilting orthogonal double prisms*, Applied Optics **53**(17), 2014, pp. 3712–3722.
- [10] YAJUN LI, *Closed form analytical inverse solutions for Risley-prism-based beam steering systems in different configurations*, Applied Optics **50**(22), 2011, pp. 4302–4309.
- [11] HAGEN N., TKACZYK T.S., *Compound prism design principles. I*, Applied Optics **50**(25), 2011, pp. 4998–5011.
- [12] YAGUANG YANG, *Analytic solution of free space optical beam steering using Risley prisms*, Journal of Lightwave Technology **26**(21), 2008, pp. 3576–3583.
- [13] ANHU LI, LIREN LIU, JIANFENG SUN, XIANGHONG ZHONG, LIJUAN WANG, DEAN LIU, ZHU LUAN, *Research on a scanner for tilting orthogonal double prisms*, Applied Optics **45**(31), 2006, pp. 8063–8069.
- [14] ANHU LI, XUCHUN JIANG, JIANFENG SUN, LIJUAN WANG, ZHIZHONG LI, LIREN LIU, *Laser coarse-fine coupling scanning method by steering double prisms*, Applied Optics **51**(3), 2012, pp. 356–364.

- [15] ANHU LI, XINJIAN GAO, WANSONG SUN, WANLI YI, YONGMING BIAN, HONGZHAN LIU, LIREN LIU, *Inverse solutions for a Risley prism scanner with iterative refinement by a forward solution*, Applied Optics **54**(33), 2015, pp. 9981–9989.
- [16] BORN M., WOLF E., *Principles of Optics*, 7th Ed., Cambridge University Press, 1999, Sec. 3.2.2.
- [17] GARCÍA-TORALES G., FLORES J.L., MUÑOZ R.X., *High precision prism scanning system*, Proceedings of SPIE **6422**, 2007, article 64220X.
- [18] ANHU LI, XUCHUN JIANG, JIANFENG SUN, YONGMING BIAN, LIJUAN WANG, LIREN LIU, *Radial support analysis for large-aperture rotating wedge prism*, Optics and Laser Technology **44**(6), 2012, pp. 1881–1888.
- [19] DILLON T.E., SCHUETZ C.A., MARTIN R.D., MACKRIDES D.G., CURT P.F., BONNETT J., PRATHER D.W., *Nonmechanical beam steering using optical phased arrays*, Proceedings of SPIE **8184**, 2011, article 81840F.

*Received February 14, 2016
in revised form April 2, 2016*